applied optics

# Design of D flip-flop and T flip-flop using Mach–Zehnder interferometers for high-speed communication

Santosh Kumar,[1,*] Gurdeep Singh,[1] Ashish Bisht,[1] and Angela Amphawan[2,3]

[1]Department of Electronics & Communication Engineering, Photonics Lab, DIT University, Dehradun-248009, India
[2]Fulbright Research Fellow, Massachusetts Institute of Technology, Cambridge, Massachusetts 02139, USA
[3]InterNetWorks Research Laboratory, School of Computing, Universiti Utara Malaysia, 06010 Sintok, Kedah, Malaysia
*Corresponding author: santoshrus@yahoo.com

Received 4 March 2015; revised 7 June 2015; accepted 12 June 2015; posted 22 June 2015 (Doc. ID 235447); published 14 July 2015

**Electrical component speed is a major constraint in high-speed communications. To overcome this constraint, electrical components are now being replaced by optical components. The application of optical switching phenomena has been used to construct the design of the D flip-flop and T flip-flop based on the electro-optic effect in a Mach–Zehnder interferometer (MZI). The MZI structures show the powerful ability to switch the optical signal from one output port to the other. Hence, it is possible to construct some complex optical combinational digital circuits using the electro-optic-effect-based MZI structure as a basic building block. This paper constitutes the mathematical description of the proposed device and thereafter compilation using MATLAB. The study is carried out by simulating the proposed device with the beam propagation method.** 

***OCIS codes:*** (230.2090) Electro-optical devices; (230.7400) Waveguides, slab; (230.3750) Optical logic devices; (250.3140) Integrated optoelectronic circuits.

http://dx.doi.org/10.1364/AO.54.006397

## 1. INTRODUCTION

Due to the ever-increasing demand for bandwidth, it is intensely challenging to scale electronic devices to greater transmission rates primarily due to their power dissipation and energy utilization. Optical packet shifting is a pleasing substitute to boost the router's forwarding speed. An essential section of any router is a memory unit, which is necessary for briefly storing the header intelligence of a packet. Optics appears as an encouraging technology for applications requiring high-speed latch and memory elements such as optical packet routing, regeneration, and ultrafast computing [1–3]. Optical flip-flops (FFs) act as the fundamental building sections [4–6], and, when mounted with other combinational circuits, can attain further sophisticated services such as shift registers, counters, D-FF, T-FF [2], and RAM cells [3]. To date, distinct optical flip-flops have been suggested based on multimode interference bistable laser diodes [7], coupled laser diodes [8], or coupled Mach–Zehnder interferometers (MZIs) [9]. An all-optical delay flip-flop is outlined employing two quantum dot (QD) semiconductor assisted MZIs, which can perform both PET and NET operations [10]. The optical bistability of a flip-flop architecture based on a single SOA-MZI with a feedback loop is studied theoretically [11,12]. The optical switching phenomenon in $LiNbO_3$-based MZIs has been studied, and its effectiveness in the implementation of various optical logic gates, combinational circuits, and routers has been shown [13–21]. Raghuwanshi *et al.* used the electro-optic-effect-based MZI structure to construct sequential logic circuits [22] in which they have implemented D flip-flop, but they have not shown $\overline{Q}_n$ in their circuit anywhere. After that, they have also shown the implementation of a 2-bit ripple counter, where they have obtained $\overline{Q}_n$ by placing a photo-detector after $Q_n$ and giving that output electrical signal to a second electrode of another MZI, which acts as an inverter), and the second output of that MZI gives us $\overline{Q}_n$. Doing so, there is a limitation in implementing any sequential logic circuit that makes use of $\overline{Q}_n$, because, as we convert $Q_n$ into an electrical signal and then apply that electrical signal to another electrode, there is a certain amount of delay to obtain $\overline{Q}_n$, due to which a limitation on the switching speed of input data ($D_n$) is imposed.

In this paper, the flip-flops are implemented with the help of MZIs by using beam propagation method (BPM), and their results are verified with the help of MATLAB and used to analyze the proposed device. The basic working principle of the feedbacked MZI, its mathematical description, and the results of the BPM have been presented in Section 2. With the help of the feedbacked MZI, D-FF and T-FF are proposed, and their

MATLAB simulation is presented in Section 3. The results obtained through the BPM and their discussions are presented in Section 4. Finally, Section 5 concludes the paper.

## 2. DESCRIPTION OF FEEDBACKED MACH–ZEHNDER INTERFEROMETER

Figure 1(a) shows the schematic diagram of a single $LiNbO_3$-based MZI with feedback. Figure 1(b) shows the schematic diagram of the delay unit applicable to the feedbacked MZI using the lithium niobate switch and the fiber loop. The numbers indicate the delay associated with each loop [22,23].

The prime function of the 1-bit delay unit is to give the state of the past output signal as feedback, so as to extract the current output. The current output depends upon the data signal applied at the second electrode of the MZI and the previous output signal states. The 1-bit delay unit time interval depends upon the data rate of the input bit stream. A hybrid optical time delay unit using lithium niobate switches with precisely produced fiber loops can be used to produce the desired amount of time delay [23]. Figure 1(b) also shows the delay unit, which can be used for the proposed device. It incorporates two lithium niobate, where each includes two $4 \times 4$ networks formed by four-directional couplers. The directional couplers are controlled by bias electrodes and single switching voltages. The $4 \times 4$ switching mechanism is joined by proper lengths of fibers, which give delay in the multiple of 44 ps [22,23]. The end faces of each die are covered with antireflection material to hold the interface reflection in check. With a view to give the large extinction ratio between delay paths, a "crosstalk avoidance" algorithm is used when a given delay path is set up. Creating the desired delay paths, the state of eight of the fourteen switch elements in the time delay unit is defined. Crosstalk introduced at each of these switches circulates through the device and couples back into the original signal path at a consecutive switch. The crosstalk signal propagates through a different group of fibers, so it will have a different delay time, due to which the extinction ratio at the output of the device is increased. As the light can couple back into the signal path due to the insufficiency of a switch set to discard it, its power level will be down by twice the crosstalk value (in decibels) for one of the switches. The described mechanism provides the desired time delay for the operation of the sequential circuits.

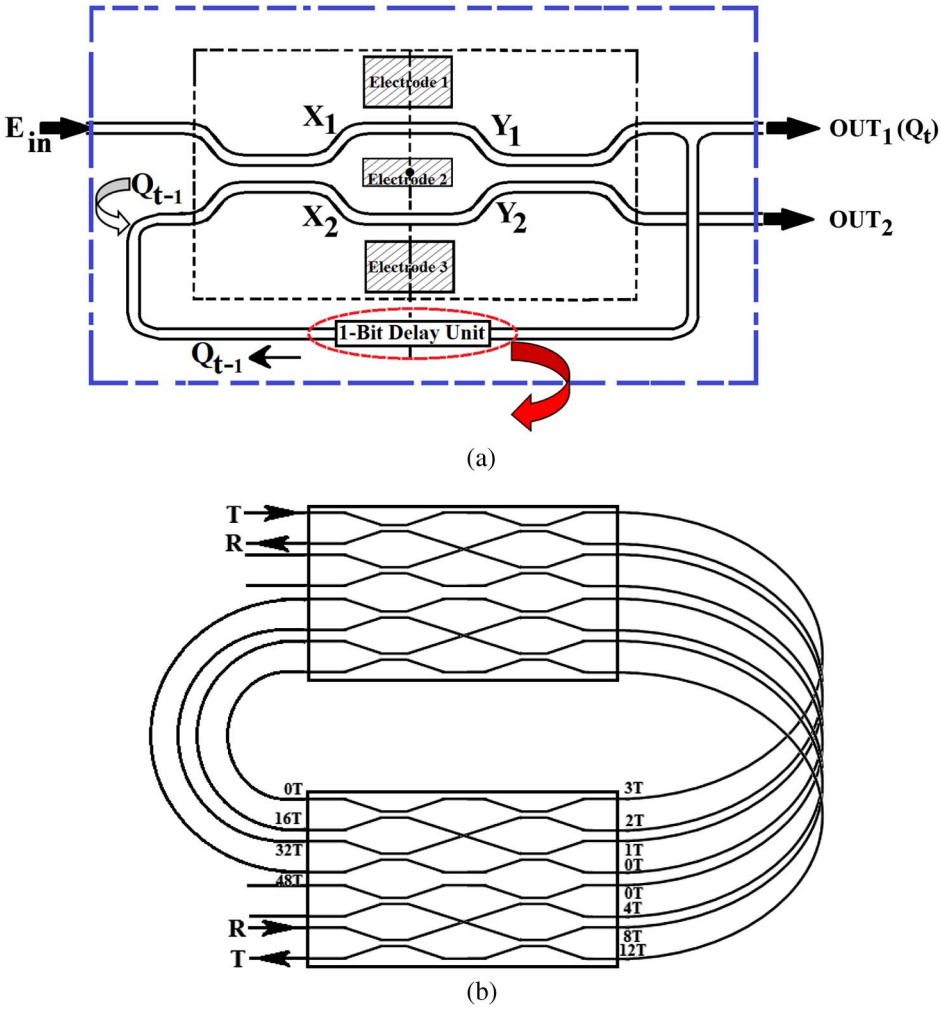


**Fig. 1.** (a) Schematic diagram of feedbacked MZI. (b) Schematic diagram of delay unit applicable to feedbacked MZI using the lithium niobate switch and the fiber loop.

From Fig. 1(a), the expression can be written as follows [17]:

$$X_1 = \sqrt{1-\alpha_1}(E_{\text{in}}) + j\sqrt{\alpha_1}(Q_{t-1}), \tag{1}$$

$$X_2 = j\sqrt{\alpha_1}(E_{\text{in}}) + \sqrt{1-\alpha_1}(Q_{t-1}), \tag{2}$$

where $\alpha_1$ is the attenuation constant of the first directional coupler represented toward the input side of Fig. 1(a). $X_1$ is the first output port of the first directional coupler, and $X_2$ is the second output port of the first directional coupler. $E_{\text{in}}$ is the optical signal applied at the first input port of the MZI, and $Q_{t-1}$ is the previous output, which is being fed at the second input port of the MZI. In matrix form, Eqs. (1) and (2) can be represented as follows:

$$\begin{bmatrix} X_1 \\ X_2 \end{bmatrix} = \begin{bmatrix} \sqrt{1-\alpha_1} & j\sqrt{\alpha_1} \\ j\sqrt{\alpha_1} & \sqrt{1-\alpha_1} \end{bmatrix} \begin{bmatrix} E_{\text{in}} \\ Q_{t-1} \end{bmatrix}. \tag{3}$$

In the same manner, we can write the expression

$$Y_1 = X_1 e^{-j\varphi_1}, \qquad Y_2 = X_2 e^{-j\varphi_2}$$

where $Y_1$ is the first input port of the second directional coupler, and $Y_2$ is the second input port of the second directional coupler. In matrix form, it can be represented as

$$\begin{bmatrix} Y_1 \\ Y_2 \end{bmatrix} = \begin{bmatrix} e^{-j\varphi_1} & 0 \\ 0 & e^{-j\varphi_2} \end{bmatrix} \begin{bmatrix} X_1 \\ X_2 \end{bmatrix}. \tag{4}$$

In the case of the second coupler, we can write the equation to obtain the output signals as follows:

$$\text{OUT}_1 = Q_t = \sqrt{1-\alpha_2}(Y_1) + j\sqrt{\alpha_2}(Y_2), \tag{5}$$

$$\text{OUT}_2 = j\sqrt{\alpha_2}(Y_1) + \sqrt{1-\alpha_2}(Y_2). \tag{6}$$

In Eqs. (5) and (6), $\alpha_2$ represents the attenuation constant of the second directional coupler, represented toward the output side of Fig. 1(a). We can represent Eqs. (5) and (6) in matrix form as follows:

$$\begin{bmatrix} \text{OUT}_1 \\ \text{OUT}_2 \end{bmatrix} = \begin{bmatrix} Q_t \\ \text{OUT}_2 \end{bmatrix} = \begin{bmatrix} \sqrt{1-\alpha_2} & j\sqrt{\alpha_2} \\ j\sqrt{\alpha_2} & \sqrt{1-\alpha_2} \end{bmatrix} \begin{bmatrix} Y_1 \\ Y_2 \end{bmatrix}. \tag{7}$$

Now substituting the value of $X_1$, $X_2$, $Y_1$ and $Y_2$ from Eqs. (3) and (4) in Eq. (7), we get

$$\begin{bmatrix} \text{OUT}_1 \\ \text{OUT}_2 \end{bmatrix} = \begin{bmatrix} Q_t \\ \text{OUT}_2 \end{bmatrix} = \begin{bmatrix} \sqrt{1-\alpha_2} & j\sqrt{\alpha_2} \\ j\sqrt{\alpha_2} & \sqrt{1-\alpha_2} \end{bmatrix} \times \begin{bmatrix} e^{-j\varphi_1} & 0 \\ 0 & e^{-j\varphi_2} \end{bmatrix} \begin{bmatrix} \sqrt{1-\alpha_1} & j\sqrt{\alpha_1} \\ j\sqrt{\alpha_1} & \sqrt{1-\alpha_1} \end{bmatrix} \begin{bmatrix} E_{\text{in}} \\ Q_{t-1} \end{bmatrix}. \tag{8}$$

Simplifying the above equation, we can write the expression for the first output port of the MZI as follows:

$$\begin{bmatrix} Q_t \\ \text{OUT}_2 \end{bmatrix} = \begin{bmatrix} \sqrt{(1-\alpha_1)(1-\alpha_2)}e^{-j\varphi_1} - \sqrt{\alpha_1\alpha_2}e^{-j\varphi_2} & j\left\{\sqrt{\alpha_1(1-\alpha_2)}e^{-j\varphi_1} + \sqrt{\alpha_2(1-\alpha_1)}e^{-j\varphi_2}\right\} \\ j\left\{\sqrt{\alpha_1(1-\alpha_2)}e^{-j\varphi_2} + \sqrt{\alpha_2(1-\alpha_1)}e^{-j\varphi_1}\right\} & -\sqrt{\alpha_1\alpha_2}e^{-j\varphi_1} + \sqrt{(1-\alpha_1)(1-\alpha_2)}e^{-j\varphi_2} \end{bmatrix} \begin{bmatrix} E_{\text{in}} \\ Q_{t-1} \end{bmatrix}.$$

Hence we can write

$$Q_t = \left[\left\{\sqrt{(1-\alpha_1)(1-\alpha_2)}e^{-j\varphi_1} - \sqrt{\alpha_1\alpha_2}e^{-j\varphi_2}\right\}E_{\text{in}} + j\left\{\sqrt{\alpha_1(1-\alpha_2)}e^{-j\varphi_1} + \sqrt{\alpha_2(1-\alpha_1)}e^{-j\varphi_2}\right\}Q_{t-1}\right]. \tag{9}$$

Here, $\varphi_1 = (\pi/V_\pi)V_1$ and $\varphi_2 = (\pi/V_\pi)V_2$. $V_\pi$ is the voltage at which the phase difference between the optical signals across the two arms of interferometers is $\pi$. In order to achieve the highest extinction ratio the attenuation constants are taken as $\alpha_1 = \alpha_2 = 0.5$ [17,18]. The extinction ratio can be represented as the ratio of the maximum and the minimum power levels of the transfer function. If the minimum power level of the transfer function is zero, we have the infinite extinction ratio. To achieve the highest extinction ratio, we require 50% of the power-splitting ratio for optical couplers [17]. Hence, ideally the couplers used in designing the device must have the attenuation constants 0.5. Hence, we can write

$$Q_t = \left[\frac{e^{-j\varphi_1} - e^{-j\varphi_2}}{2}\right]E_{\text{in}} + \left[j\frac{\{e^{-j\varphi_1} + e^{-j\varphi_2}\}}{2}\right]Q_{t-1}$$

$$Q_t = \left[\frac{e^{-j((\varphi_1+\varphi_2+\varphi_1-\varphi_2)/2)} - e^{-j((\varphi_1+\varphi_2-\varphi_1+\varphi_2)/2)}}{2}\right]E_{\text{in}} + \left[j\frac{\{e^{-j((\varphi_1+\varphi_2+\varphi_1-\varphi_2)/2)} + e^{-j((\varphi_1+\varphi_2-\varphi_1+\varphi_2)/2)}\}}{2}\right]Q_{t-1}$$

$$Q_t = e^{-j(\varphi_1+\varphi_2)/2}\left[\frac{e^{-j(\varphi_1-\varphi_2)/2} - e^{j(\varphi_1-\varphi_2)/2}}{2}\right]E_{\text{in}} + je^{-j(\varphi_1+\varphi_2)/2}\left[\frac{e^{-j(\varphi_1-\varphi_2)/2} + e^{j(\varphi_1-\varphi_2)/2}}{2}\right]Q_{t-1}.$$

We assume that $(\varphi_1 + \varphi_2)/2) = \varphi_0$ and $(\varphi_1 - \varphi_2) = \Delta\varphi$. In the same manner, we can write

$$Q_t = e^{-j\varphi_0}\left[\left\{\frac{e^{-j(\Delta\varphi/2)} - e^{j(\Delta\varphi/2)}}{2}\right\}E_{\text{in}} + j\left\{\frac{e^{-j(\Delta\varphi/2)} + e^{j(\Delta\varphi/2)}}{2}\right\}Q_{t-1}\right], \tag{10}$$

$$Q_t = e^{-j\varphi_0}\left[-j\sin\left(\frac{\Delta\varphi}{2}\right)E_{\text{in}} + j\cos\left(\frac{\Delta\varphi}{2}\right)Q_{t-1}\right]$$

$$|Q_t|^2 = \sin^2\left(\frac{\Delta\varphi}{2}\right)|E_{\text{in}}|^2 + \cos^2\left(\frac{\Delta\varphi}{2}\right)|Q_{t-1}|^2 + |E_{\text{in}}||Q_{t-1}|\sin(\Delta\varphi). \tag{11}$$

Figure 2 shows the simulation results of the single MZI with feedback obtained for different values of control signals applied to the second electrode of the MZI.

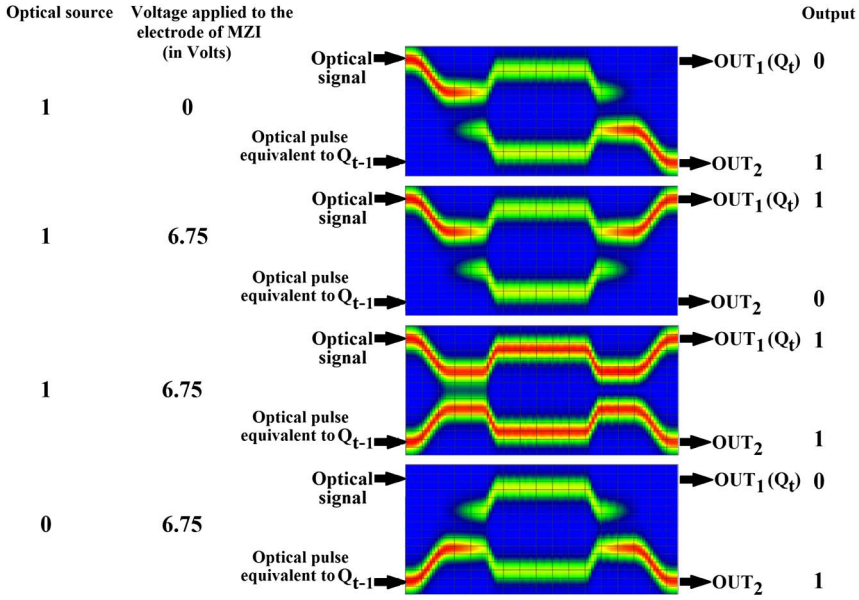


**Fig. 2.** Results of the single feedbacked MZI with feedback for different values of control signal obtained through the BPM.

## 3. DESIGN OF D AND T FLIP-FLOPS USING MZIS

The application of flip-flops is essential in order to improve the flexibility in complex sequential logic circuits. Many researchers have shown their interest to implement an all-optical flip-flop using SOA-MZIs, but SOA-MZIs have a major drawback of gain saturation.

### A. Design of D Flip-Flop

Figure 3 shows the schematic diagram of the D flip-flop using MZIs. Here, an optical signal is given to the first input port of MZI1. The first output port of MZI1 is connected to the first input port of MZI3. After that, the first output port of MZI3 is considered as $Q_n$ (present output of flip-flop), and then it is fed back into the second input port of MZI3 using a 1-bit delay element. Similarly, the second output port of MZI1 is connected to the first input port of MZI2, the first output port of which is taken as $\overline{Q}_n$ (present complement output), and it is fed back into the second input port of MZI2 using a 1-bit delay element. Data ($D_n$) is given as the control signal to the second electrode of MZI1, and clock (CLK) is given as the control signal to the second electrodes of MZI2 and MZI3.

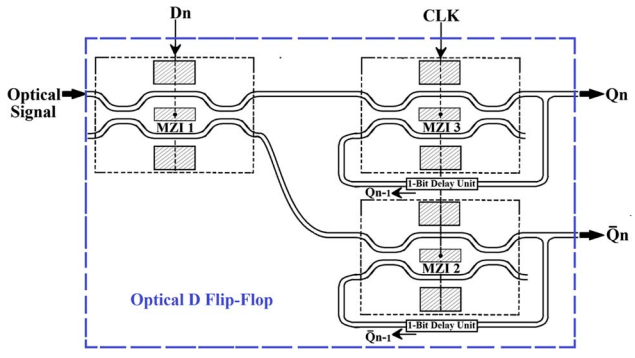


**Fig. 3.** Schematic diagram of D flip-flop.

For feedbacked MZI3 (in Fig. 3), using the relation of the single stage feedbacked MZI structure from Eqs. (10), we can write the expression for the output of the D flip-flop as follows:

$$Q_n = e^{-j\varphi_0}\left[\left\{\frac{e^{-j(\Delta\varphi/2)} - e^{j(\Delta\varphi/2)}}{2}\right\}D_n + j\left\{\frac{e^{-j(\Delta\varphi/2)} + e^{j(\Delta\varphi/2)}}{2}\right\}Q_{n-1}\right], \tag{12}$$

$$\begin{aligned} Q_n &= e^{-j\varphi_0}\left[-j\sin\left(\frac{\Delta\varphi}{2}\right)D_n + j\cos\left(\frac{\Delta\varphi}{2}\right)Q_{n-1}\right]|Q_n|^2 \\ &= \sin^2\left(\frac{\Delta\varphi}{2}\right)|D_n|^2 + \cos^2\left(\frac{\Delta\varphi}{2}\right)|Q_{n-1}|^2 \\ &\quad + |D_n||Q_{n-1}|\sin\Delta\varphi. \end{aligned} \tag{13}$$

Similarly for $\overline{Q}_n$ we can write

$$|\overline{Q}_n|^2 = \sin^2\left(\frac{\Delta\varphi}{2}\right)|\overline{D}_n|^2 + \cos^2\left(\frac{\Delta\varphi}{2}\right)|\overline{Q}_{n-1}|^2 + |\overline{D}_n||\overline{Q}_{n-1}|\sin(\Delta\varphi). \tag{14}$$

The function table of the D flip-flop is shown in Table 1. It is clear from the table that when the clock signal arrives, the data that are applied to the D-input of the flip-flop appear at the output $Q_n$ of the flip-flop, and when there is no clock signal, previous data appear at the output. The function table is verified by the BPM simulation results shown in Fig. 8.

**Table 1. Function Table of D Flip-Flop**

| $D_n$ | CLK | $Q_n$ | $\overline{Q}_n$ |
|---|---|---|---|
| 0 | 1 | 0 | 1 |
| 1 | 1 | 1 | 0 |
| × | 0 | Last $Q_n$ | Last $\overline{Q}_n$ |

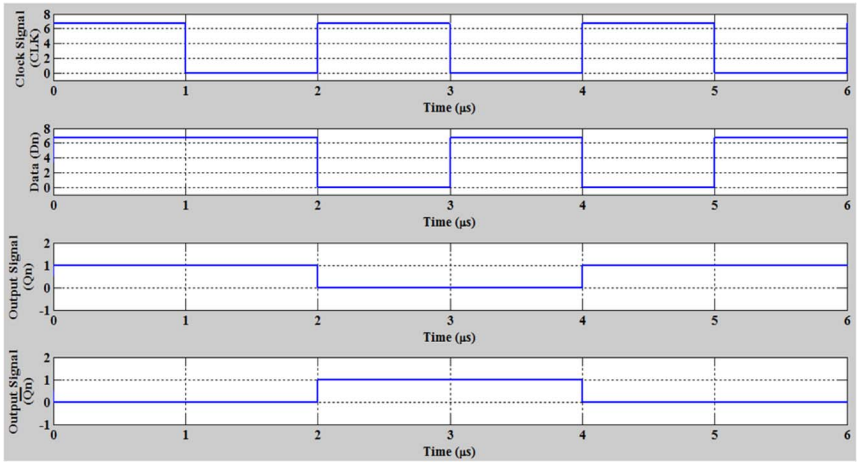


**Fig. 4.** MATLAB simulation result of D flip-flop.

Figure 4 shows MATLAB simulation results of the D flip-flop, where the first row represents the CLK signal, which acts as a control signal applied to the second electrode of MZI2 and MZI3. The second row represents the data signal, which acts as a control signal applied to the second electrode of MZI1. Similarly, the third and fourth rows represent the output signal ($Q_n$) and the complement output signal ($\overline{Q}_n$).

### B. Design of T Flip-Flop

Figure 5 shows the schematic diagram of the T flip-flop using MZIs. Here, an optical signal is given to the first input port of MZI1, the first output port of which is connected to the first input port of MZI2. Similarly, the second output port of MZI1 is connected to the second input of MZI2. The first output port of MZI2 is connected to the first input port of MZI4, the first output port of which is taken as $Q_m$, and then this $Q_m$ (present output of T flip-flop) is fed back into the second input port of MZI4 using a 1-bit delay element. The second output port of MZI2 is connected to the first input port of MZI3, the first output port of which is taken as $\overline{Q}_m$ (present complement output of T-flip-flop), which is then fed back into the second input port of MZI3. Toggle signal ($T_m$) is given as the control signal to the second electrode of MZI1. The complement output $\overline{Q}_m$ is provided to a PIN photo-detector via a 1-bit delay element, which converts the optical signal to an electrical signal, which is given to the amplifier, which amplifies the signal obtained from the photo-detector, and then this electrical signal is given as the control signal to the second electrode of MZI2. Clock (CLK) is given as the control signal to the second electrodes of MZI3 and MZI4.

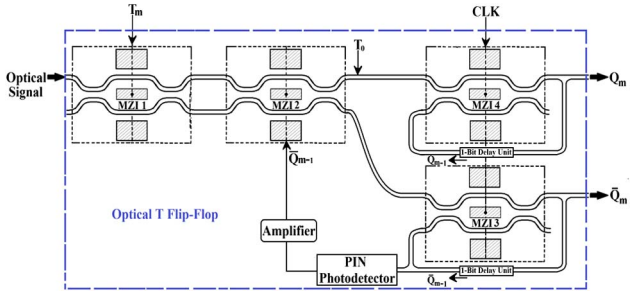


**Fig. 5.** Schematic diagram of T flip-flop using MZIs.

For the T flip-flop (as shown in Fig. 5), the combination of MZI1 and MZI2 constitutes the X-NOR and XOR logic gates. The first and second output ports of MZI2 provide X-NOR and XOR logic, respectively. So, the mathematical expression for the first output port of MZI2 can be written as follows [16]:

$$T_0 = \sin^2\left(\frac{\Delta\varphi_{\mathrm{MZI1}}}{2}\right)\sin^2\left(\frac{\Delta\varphi_{\mathrm{MZI2}}}{2}\right) + \cos^2\left(\frac{\Delta\varphi_{\mathrm{MZI1}}}{2}\right)\cos^2\left(\frac{\Delta\varphi_{\mathrm{MZI2}}}{2}\right)$$
$$T_0 = (T_m)\odot(\overline{Q}_{m-1}). \tag{15}$$

Similarly for the second output port of MZI2 the mathematical expression can be written as follows [16]:

$$\overline{T}_0 = \cos^2\left(\frac{\Delta\varphi_{\mathrm{MZI1}}}{2}\right)\sin^2\left(\frac{\Delta\varphi_{\mathrm{MZI2}}}{2}\right) + \sin^2\left(\frac{\Delta\varphi_{\mathrm{MZI1}}}{2}\right)\cos^2\left(\frac{\Delta\varphi_{\mathrm{MZI2}}}{2}\right)$$
$$\overline{T}_0 = (T_m)\oplus(\overline{Q}_{m-1}). \tag{16}$$

For feedbacked MZI4 (in Fig. 5), using the relation of the single stage feedbacked MZI structure from Eqs. (10), finally, we can write the expression for the output of the T flip-flop from feedbacked MZI4 by using Eq. (10);

$$|Q_m|^2 = \sin^2\left(\frac{\Delta\varphi}{2}\right)|T_0|^2 + \cos^2\left(\frac{\Delta\varphi}{2}\right)|Q_{m-1}|^2 + |T_0||Q_{m-1}|\sin(\Delta\varphi). \tag{17}$$

Similarly for $\overline{Q}_m$ we can write

$$|\overline{Q}_m|^2 = \sin^2\left(\frac{\Delta\varphi}{2}\right)|\overline{T}_0|^2 + \cos^2\left(\frac{\Delta\varphi}{2}\right)|\overline{Q}_{m-1}|^2 + |\overline{T}_0||\overline{Q}_{m-1}|\sin(\Delta\varphi). \tag{18}$$

The function table of the T flip-flop is shown in Table 2. It is clear from the table that when the $T_m$ input is equal to 0,

**Table 2. Function Table of T Flip-Flop**

| $T_m$ | $Q_m$ | $Q_{m+1}$ | $\overline{Q}_m$ | $\overline{Q}_{m+1}$ |
|---|---|---|---|---|
| 0 | 0 | 0 | 1 | 1 |
| 0 | 1 | 1 | 0 | 0 |
| 1 | 0 | 1 | 1 | 0 |
| 1 | 1 | 0 | 0 | 1 |

previous data $Q_m$ remains at the output of the flip-flop, and when the T-input is changed to 1, $Q_m$ gets toggled. The function table is verified by the BPM simulation results shown in Fig. 10.

Figure 6 shows the MATLAB simulation results of the T flip-flop, where the first row represents the CLK signal, which acts as a control signal applied to the second electrode of MZI3 and MZI4. The second row represents the toggle signal ($T_m$), which acts as a control signal applied to the second electrode of MZI1. The third row represents the output signal ($Q_m$), and the fourth row represents the complement output signal ($\overline{Q}_m$).

## 4. DESIGN OF D AND T FLIP-FLOPS USING BPM

Further extending, OptiBPM is used to analyze the proposed structures [13–22]. OptiBPM basically works on the principle of the finite difference beam propagation method (FD-BPM) and provides complete information of the optical waveguide depending upon its refractive index profile, structure, and material used for construction of the optical waveguide. The radiation and the guided field can be examined simultaneously.

### A. Design of D Flip-Flop

The layout of the D flip-flop consists of three MZIs as shown in Fig. 7. Here, an optical signal is given to input 1 of MZI1. The output port 1 of MZI1 is connected to the first input port of MZI3. The first output port of MZI3 is considered as $Q_n$. The second output port of MZI1 is connected to the first input port of MZI2. The first output port of MZI2 is taken as $\overline{Q}_n$. Data ($D_n$) is given as the control signal to the second electrode of the first MZI, and clock (CLK) is given as the control signal to the second electrode of MZI2 and MZI3.

Depending on the combination of input data ($D_n$) and clock signal (in the form of voltages applied at electrodes of MZIs), the output ($Q_n$) will vary. The different combinations of control signals are applied to the proposed device as shown in Fig. 8, and its corresponding responses can be discussed as follows.

Case 1: ($D_n = 1$, Clock $= 1$)

As the data signal ($D_n$) is equal to 1 (i.e., 6.75 V is being applied to the second electrode of MZI1), the light emerges out of the first output port of MZI1 and goes to the first input port of MZI3. It is also given that the clock signal is equal to 1, meaning that 6.75 V voltage is applied to the second electrode of MZI2 and MZI3. But light is only entering from the first input port of MZI3; output light will only come out of the first output port of MZI3, which is $Q_n$. So, $Q_n = 1$ and $\overline{Q}_n = 0$ (as shown in Fig. 8).

Case 2: ($D_n = 1$, Clock $= 0$)

In this case, the data signal is kept at 1, but the clock signal is varied from 1 to 0 (meaning that the voltage at the second electrode of MZI3 is varied from 6.75 to 0 V), due to which the light signal appears at the first output port of MZI1, enters the first input port of MZI3, and then comes out of the flip-flop from the second output port of MZI3 (as shown in Fig. 3). Also, due to the 1-bit delay element introduced between the first output port of MZI3 and the second input port of MZI3, the previous $Q_n$ is given back to the second input port of MZI3. Due to the clock being set at 0, the fed back $Q_n$ emerges out of the first output port of MZI3 (as shown in Fig. 8).

Case 3: ($D_n = 0$, Clock $= 1$)

In this case, the data signal is varied from 1 to 0, and the clock signal is set at 1. As the voltage applied to the second electrode of MZI1 is set equal to 0 V, the light signal (which is constantly being fed to the first input port of MZI1) comes out of the second output port of MZI1 and enters the first

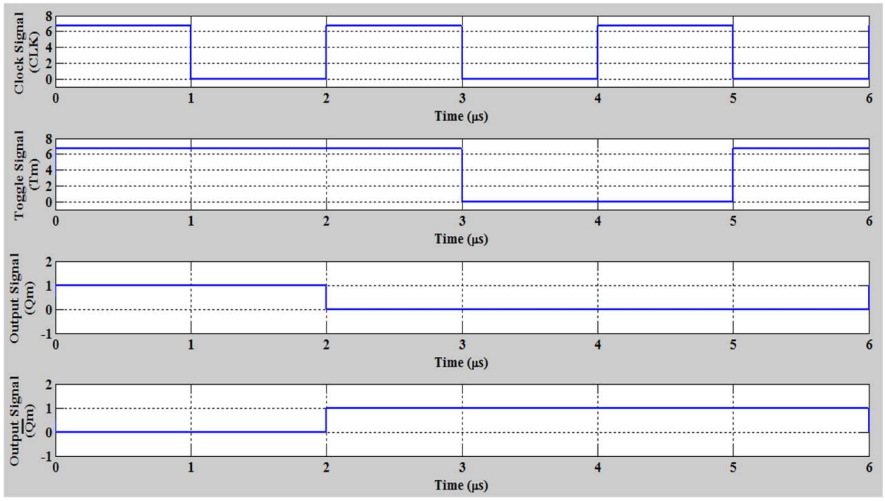


**Fig. 6.** MATLAB simulation results of T flip-flop.

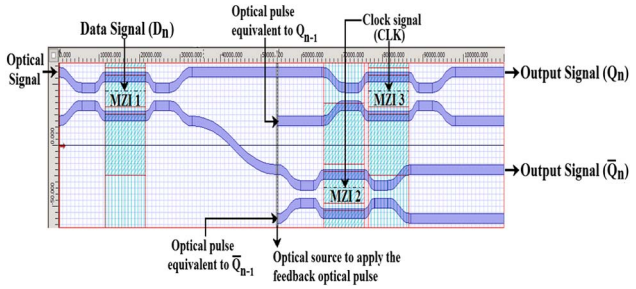


**Fig. 7.** Layout diagram of D flip-flop using three MZIs.

input port of MZI2. Since the clock signal is set equal to 1 for the present case, light will come out of the first output port of MZI2, which is $\overline{Q}_n$. At the same time, due to the feedback applied between the first output port of MZI3 and the second input port of MZI3 through the 1-bit delay element, a previous value of $Q_n$ comes at that port (which is equal to 1 in the previous case, i.e., case 2). Feedback light comes out of the second output port of MZI3 because 6.75 V is applied to the second electrode of MZI3. So, $Q_n = 0$ and $\overline{Q}_n = 1$ (as shown in Fig. 8).

Case 4: ($D_n = 1$, Clock $= 0$)

In this case, the data signal is set back to 1 (i.e., 6.75 V is applied to the second electrode of MZI1). Due to this, light comes out of the first output port of MZI1 and enters the first input of MZI3, which further comes out of MZI3 at the second output port because of the clock signal set at 0. At the same time, due to the feedback applied between the first output port of MZI2 and the second input port of MZI2 through the 1-bit delay element, the previous value of $\overline{Q}_n$ comes at that port (which is equal to 1 in the previous case, i.e., case 3). Since the clock signal is set equal to 0, feedback light comes out of the first output port of MZI2. So, $Q_n = 0$ and $\overline{Q}_n = 1$ (as shown in Fig. 8).

Case 5: ($D_n = 0$, Clock $= 0$)

In this case, the data signal is again set back to 0. Due to this, light appears at the second output port of MZI1, enters the first input port of MZI2, and then comes out of the second output port of MZI2 because 0 V is applied to the second electrode of MZI2. At the same time, the previous $Q_n$ is being fed back to the second input port of MZI3, which comes out of the first output port of MZI3 because 0 V is applied to the second electrode of MZI3 resulting in $Q_n = 1$ and $\overline{Q}_n = 0$ (as shown in Fig. 8).

Case 6: ($D_n = 1$, Clock $= 1$)

In this case, once again the data signal is kept at 1 (meaning thereby 6.75 V is applied to the second electrode of MZI1). Due to this, light comes out of the first output port of MZI1 and appears at the first input port of MZI3, which further comes out of the first output port of MZI3 because 6.75 V is applied to the second electrode of MZI3 (i.e., the clock signal is equal to 1). At the same time, the previous $Q_n$ (= 1) is fed back into the second input port of MZI3, which comes out of the second output port (because 6.75 V is applied to the second electrode of MZI3). So, $Q_n = 1$ and $\overline{Q}_n = 0$ (as shown in Fig. 8).

### B. Design of T Flip-Flop

The BPM layout diagram of the $T$ flip-flop is shown in Fig. 9. Here, the control signals are arranged similarly to the previous case. As shown in Fig. 5, light input is constantly being fed to the first input of MZI1. Toggle signal ($T_m$) is applied to the second electrode of MZI1. Similarly, the clock signal is applied to the second electrodes of MZI3 and MZI4. $\overline{Q}_{m-1}$ (voltage equivalent of previous light signal from first output port of MZI3) is applied to the second electrode of MZI2. Depending on the values of voltage signals that are being applied to the electrodes of four MZIs, the output light signals ($Q_m$ and $\overline{Q}_m$) will vary.

The result of the T flip-flop obtained from the BPM is shown in Fig. 10. It can be verified by Table 2, which is the truth table of the T flip-flop obtained from MATLAB (as shown in Fig. 6). The different combinations of control signals are applied to the proposed device as shown in Fig. 10, and its corresponding responses can be discussed as follows.

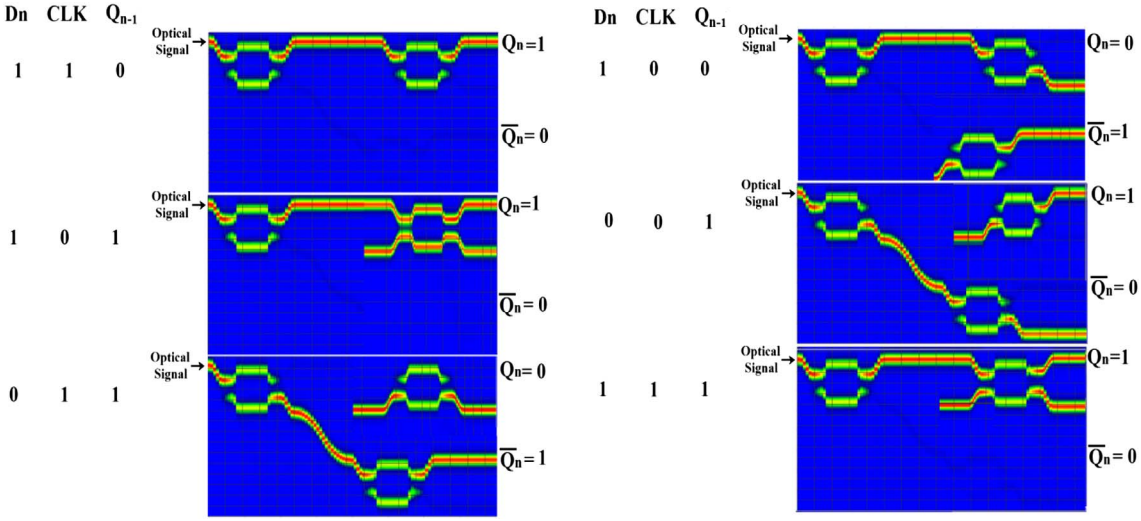


**Fig. 8.** Results of the D flip-flop for different combinations of control signals obtained through the BPM.

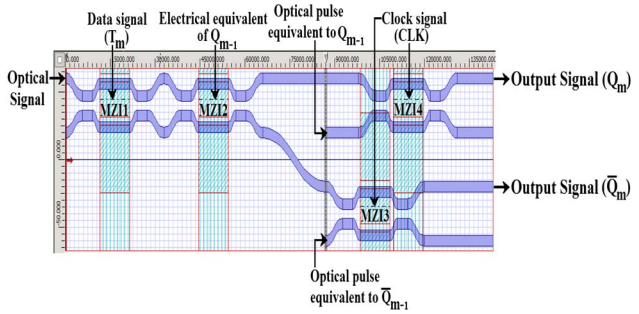


**Fig. 9.** Layout diagram of T flip-flop using MZIs.

Case 1: ($T_m = 1, \overline{Q}_{m-1} = 1, \text{Clock} = 1$)

In this case, the $T_m$ (Toggle) signal is set equal to 1 (meaning thereby 6.75 V voltage is applied to the second electrode of MZI1), due to which light comes out of the first output port of MZI1 and appears at the first input port of MZI2. Also, $\overline{Q}_{m-1}$ is equal to 6.75 V. So, the light signal appearing at the first input port of MZI2 will come out from its first output port and appear at the first input port of MZI4. Since the clock signal is also set equal to 1, light will emerge out of the first output of MZI4, which is $Q_m$. At the same time, the previous $\overline{Q}_m$ that is being fed back into the input port of MZI3 comes out of the second input port of MZI3 because 6.75 V voltage is applied to its second electrode (clock signal is set equal to 1). So, $Q_m = 1$ and $\overline{Q}_m = 0$ (as shown in Fig. 10).

Case 2: ($T_m = 1, \overline{Q}_{m-1} = 0, \text{Clock} = 0$)

In this case, the $T_m$ (Toggle) signal is kept at 1, due to which light comes out of the first output port of MZI1, enters the first input port of MZI2, and then comes out from its second output port (because $\overline{Q}_m$ in case 1 was equal to 0). This light signal appears at the first input port of MZI3. Since the clock signal is equal to zero, the light signal emerges out of the second output port of MZI3. At the same time, the light signal (i.e., $Q_m = 1$ in case 1) that is being fed back from the first output port of MZI4 using a delay element again comes out of the first output port of MZI4, because 0 V (clock signal = 0) is applied at the second electrode of MZI4. So, $Q_m = 1$ and $\overline{Q}_m = 0$ (as shown in Fig. 10).

Case 3: ($T_m = 1, \overline{Q}_{m-1} = 0, \text{Clock} = 1$)

In this case, the $T_m$ (Toggle) signal is again kept at 1, due to which light comes out of the first output port of MZI1, enters the first input port of MZI2, and then comes out from its second output port (because $\overline{Q}_m$ in case 2 was equal to 0). This light signal appears at the first input port of MZI3. Since the clock signal is equal to 1, the light signal emerges out of the first output port of MZI3. At the same time, the light signal (i.e., $Q_m = 1$ in case 2) that is being fed back from the first output port of MZI4 into the second input port of MZI4 using a delay element comes out of the second output port of MZI4, because 6.75 V (clock signal = 1) is applied at the second electrode of MZI4. So, $Q_m = 0$ and $\overline{Q}_m = 1$ (as shown in Fig. 10).

Case 4: ($T_m = 0, \overline{Q}_{m-1} = 1, \text{Clock} = 0$)

In this case, the $T_m$ (Toggle) signal is varied from 1 to 0 (i.e., voltage at second electrode of MZI1 is varied from 6.75 to 0 V), due to which light emerges out of the second output port of MZI1, appears at the second input port of MZI2, and then comes out of the second output port of MZI2 (because $\overline{Q}_m$ in case 3 was equal to 1). This light signal enters the first input port of MZI3. Since the clock signal is equal to 0, the light signal emerges out of the second output port of MZI3. At the same time, the light signal (i.e., $\overline{Q}_m = 1$ in case 3) that is being fed back from the first output port of MZI3 back into the second input port of MZI3 using a delay element again comes out of the first output port of MZI3, because 0 V (clock signal = 0) is applied at the second electrode of MZI3. So, $Q_m = 0$ and $\overline{Q}_m = 1$ (as shown in Fig. 10).

Case 5: ($T_m = 0, \overline{Q}_{m-1} = 1, \text{Clock} = 1$)

In this case, the $T_m$ (Toggle) signal is kept at 0 (i.e., voltage at second electrode is 0 V), due to which light emerges out of the second output port of MZI1, appears at the second input port of MZI2, and then comes out from its second output port (because $\overline{Q}_m$ in case 4 was equal to 1). This light signal enters the first input port of MZI3. Since the clock signal is equal to 1, the light signal emerges out of the first output port of MZI3. At the same time, the light signal (i.e., $\overline{Q}_m = 1$ in case 4) that is being fed back from the first output port of MZI3 into the second input port of MZI3 using a delay element comes

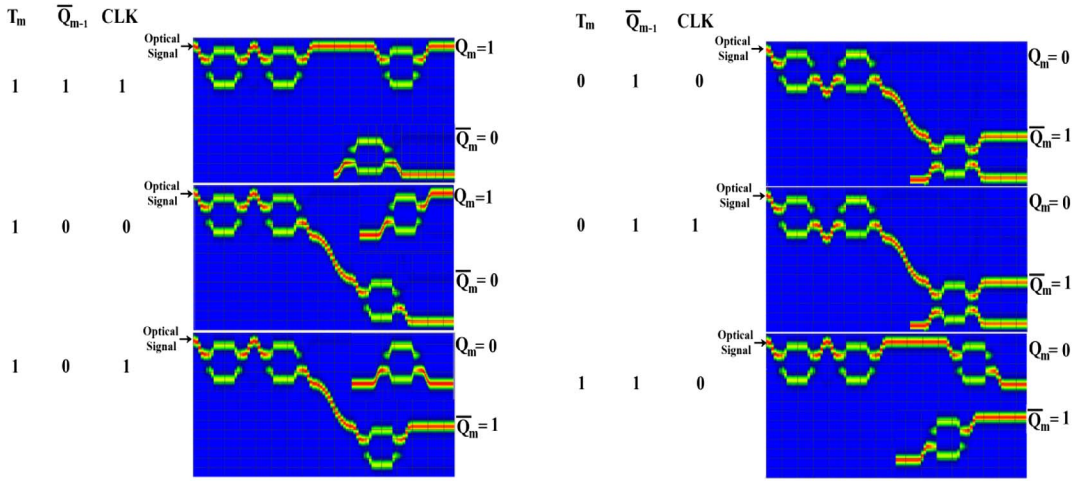


**Fig. 10.** Results of the T flip-flop for different combinations of control signals obtained through the BPM.

out of the second output port of MZI3, because 6.75 V (clock signal = 1) is applied at the second electrode of MZI3. So, $Q_m = 0$ and $\overline{Q}_m = 1$ (as shown in Fig. 10).

Case 6: ($T_m = 1, \overline{Q}_{m-1} = 1, \text{Clock} = 0$)

$T_m$ (Toggle) signal is again varied from 0 to 6.75 V, due to which the light signal comes out of the first output port of MZI1, appears at the first input port of MZI2, and then comes out from its first output port of MZI2 (because $\overline{Q}_m$ is equal to 1 in case 5). Then, this light comes out of the second output port of MZI4 because the clock signal is set equal to 0 V. At the same time, the light signal (i.e., $\overline{Q}_m = 1$ in case 5) that is being fed back from the first output port of MZI3 back into the second input port of MZI3 using a delay element comes out of the first output port of MZI3, because 0 V (clock signal = 0) is applied at the second electrode of MZI3. So, $Q_m = 0$ and $\overline{Q}_m = 1$ (as shown in Fig. 10).

## 5. CONCLUSION

The proposed devices are discussed with appropriate mathematical analysis, and the results are obtained using MATLAB simulation. The discussed method is verified using the BPM. The paper includes detailed discussion of the flip-flop. It presents the guideline to realize D-flip-flop and T-flip-flop by using feedbacked MZIs. The proposed scheme would be a promising basic building module in optical networks and computing systems for complex operations. The results furnished in this paper will be a stepping stone in the area of designing DWDM optical components for optical network systems.

**Funding.** DIT University, India (DITU/R&D/2014/7/ECE).

**Acknowledgment.** The authors thank Prof. K. K. Raina, Vice-Chancellor, DIT University, India, for encouragement and support during the present research work. The authors also thank the anonymous reviewers for their constructive suggestions.

## REFERENCES

1. P. Bakopoulos, P. Zakynthinos, E. Kehayas, L. Stampoulidis, F. Fresi, C. Porzi, N. Calabretta, C. Stamatiadis, Ch. Kouloumentas, D. Petrantonakis, A. Maziotis, D. Apostolopoulos, M. Guina, D. Klonidis, L. Potì, E. Tangdiongga, A. Poustie, G. Maxwell, I. Tomkos, A. Bogoni, H. J. S. Dorren, and H. Avramopoulos, "160 Gb/s all-optical contention resolution with prioritization using integrated photonic components," in *Proceedings of the 34th European Conference on Optical Communication*, Vienna, Austria (2009).
2. J. Wang, G. Meloni, G. Berettini, L. Poti, and A. Bogoni, "All-optical clocked flip-flops and binary counting operation using SOA-based SR latch and logic gates," IEEE J. Sel. Top. Quantum Electron. **16**, 1486–1494 (2010).
3. N. Pleros, D. Apostolopoulos, D. Petrantonakis, C. Stamatiadis, and H. Avramopoulos, "Optical static RAM cell," IEEE Photon. Technol. Lett. **21**, 73–75 (2009).
4. Y. Liu, R. McDougall, M. T. Hill, G. D. Maxwell, S. Zhang, R. Harmon, F. M. Huijskens, L. Rivers, H. J. S. Dorren, and A. Poustie, "Packaged and hybrid integrated all-optical flip-flop memory," Electron. Lett. **42**, 1399–1400 (2006).
5. M. T. Hill, "A fast low-power optical memory based on coupled micro-ring lasers," Nature **432**, 206–209 (2004).
6. L. Liu, R. Kumar, K. Huybrechts, T. Spuesens, G. Roelkens, E. J. Geluk, T. de Vries, P. Regreny, D. V. Thourhout, R. Baets, and G. Morthier, "An ultra-small, low-power, all-optical flip-flop memory on a silicon chip," Nature **268**, 1–6 (2010).
7. M. Takenaka, K. Takeda, Y. Kanema, Y. Nakano, M. Raburn, and T. Miyahara, "All-optical switching of 40 Gb/s packets by MMI-BLD optical label memory," Opt. Express **14**, 10785–10789 (2006).
8. M. T. Hill, H. de Waardt, G. D. Khoe, and H. J. S. Dorren, "All-optical flip-flop based on coupled laser diodes," IEEE J. Quantum Electron. **37**, 405–413 (2001).
9. M. T. Hill, H. J. S. Dorren, X. J. M. Leijtens, J. H. den Besten, T. de Vries, J. H. C. van Zantvoort, E. Smalbrugge, Y. S. Oei, J. J. M. Binsma, G. D. Khoe, and M. K. Smit, "Coupled Mach-Zehnder interferometer memory element," Opt. Lett. **30**, 1710–1712 (2005).
10. E. Kehayas, J. Seoane, Y. Liu, J. M. Martinez, J. Herrera, P. V. Holm-Nielsen, S. Zhang, R. McDougall, G. Maxwell, F. Ramos, J. Marti, H. J. S. Dorren, P. Jeppesen, and H. Avramopoulos, "All-optical network subsystems using integrated SOA-based optical gates and flip-flops for label-swapped networks," IEEE Photon. Technol. Lett. **18**, 1750–1752 (2006).
11. T. Chattopadhyay and D. Kumar Gayen, "Reconfigurable all-optical delay flip-flop using QD-SOA assisted Mach–Zehnder interferometer," J. Lightwave Technol. **32**, 4571–4577 (2014).
12. R. Clavero, F. Ramos, and J. Martí, "Bistability analysis for optical flip-flops based on a SOA-MZI with feedback," J. Lightwave Technol. **25**, 3641–3648 (2007).
13. S. Kumar, S. K. Raghuwanshi, and A. Kumar, "Implementation of optical switches by using Mach-Zehnder interferometer," Opt. Eng. **52**, 097106 (2013).
14. S. Kumar, S. K. Raghuwanshi, and A. Kumar, "1 × 8 signal router using cascading the Mach-Zehnder interferometers," in *6th IEEE/International Conference on Advanced Infocomm Technology* (IEEE/ICAIT, 2013), pp. 161–162.
15. S. Kumar, A. Kumar, and S. K. Raghuwanshi, "Implementation of an optical AND gate using Mach-Zehnder interferometers," Proc. SPIE **9131**, 913120 (2014).
16. A. Kumar, S. Kumar, and S. K. Raghuwanshi, "Implementation of XOR/XNOR and AND logic gates using Mach-Zehnder interferometers," Optik **125**, 5764–5767 (2014).
17. S. K. Raghuwanshi, A. Kumar, and S. Kumar, "1 × 4 signal router using 3-Mach-Zehnder interferometers," Opt. Eng. **52**, 035002 (2013).
18. A. Kumar, S. Kumar, and S. K. Raghuwanshi, "Implementation of full-adder and full-subtractor based on electro-optic effect in Mach-Zehnder interferometer," Opt. Commun. **324**, 93–107 (2014).
19. A. Kumar and S. K. Raghuwanshi, "Implementation of optical gray code converter and even parity checker using the electro-optic effect in the Mach–Zehnder interferometer," Opt. Quantum Electron., doi: 10.1007/s11082-014-0087-9 (to be published).
20. S. Kumar, A. Bisht, G. Singh, K. Choudhary, and D. Sharma, "Implementation of wavelength selector based on electro-optic effect in Mach-Zehnder interferometers for high speed communications," Opt. Commun. **350**, 108–118 (2015).
21. S. Kumar, G. Singh, and A. Bisht, "4 × 4 signal router based on electro-optic effect of Mach-Zehnder interferometer for wavelength division multiplexing applications," Opt. Commun. **353**, 17–26 (2015).
22. S. K. Raghuwanshi, A. Kumar, and N. K. Chen, "Implementation of sequential logic circuits using the Mach–Zehnder interferometer structure based on electro-optic effect," Opt. Commun. **333**, 193–208 (2014).
23. E. J. Murphy, T. F. Adda, W. J. Minford, R. W. Irvin, E. I. Ackerman, and S. B. Adam, "Guided-wave optical time delay network," IEEE Photon. Technol. Lett. **8**, 545–547 (1996).